

# Dynamic formation of quasicondensate and spontaneous vortices in a strongly interacting Fermi gas

Xiang-Pei Liu<sup>1,2,3,\*</sup>, Xing-Can Yao<sup>1,2,3,\*</sup>, Youjin Deng<sup>1,2,3,6,\*</sup>, Yu-Xuan Wang<sup>1,2,3</sup>, Xiao-Qiong Wang<sup>1,2,3</sup>, Xiaopeng Li<sup>4,5</sup>, Qijin Chen<sup>1,2,3</sup>, Yu-Ao Chen<sup>1,2,3</sup>, and Jian-Wei Pan<sup>1,2,3</sup>

<sup>1</sup>Hefei National Laboratory for Physical Sciences at the Microscale and Department of Modern Physics, University of Science and Technology of China, Hefei 230026, China

<sup>2</sup>Shanghai Branch, CAS Center for Excellence in Quantum Information and Quantum Physics, University of Science and Technology of China, Shanghai 201315, China

<sup>3</sup>Shanghai Research Center for Quantum Sciences, Shanghai 201315, China

<sup>4</sup>State Key Laboratory of Surface Physics, Institute of Nanoelectronics and Quantum Computing, and Department of Physics, Fudan University, Shanghai 200433, China

<sup>5</sup>Collaborative Innovation Center of Advanced Microstructures, Nanjing 210093, China and

<sup>6</sup>MinJiang Collaborative Center for Theoretical Physics,

College of Physics and Electronic Information Engineering, Minjiang University, Fuzhou 350108, China

(Dated: December 20, 2021)

We report an experimental study of quench dynamics across the superfluid transition temperature  $T_c$  in a strongly interacting Fermi gas by ramping down the trapping potential. The nonzero quasi-condensate number  $N_0$  at temperature significantly above  $T_c$  in the unitary and the BEC regimes reveals the pseudogap physics. Below  $T_c$ , a rapid growth of  $N_0$  is accompanied by spontaneous generation of tens of vortices. We observe a power law scaling of the vortex density versus the quasi-condensate formation time, consistent with the Kibble-Zurek theory. Our work provides an example of studying emerged many-body physics by quench dynamics and paves the way for studying the quantum turbulence in a strongly interacting Fermi gas.

In pursuit of correlated quantum physics in strongly interacting Fermi gases, great efforts have been devoted to studying equilibrium phases and transitions [1–6]. This has shed light on the understanding of high- $T_c$  superconductivity [7–9] and the modeling of equation of states of dense neutron stars [10]. Of equal importance would be to probe the non-equilibrium dynamics during a temperature quench across the superfluid transition temperature  $T_c$ , where the superfluid growth is closely connected to the generation of spontaneous vortices.

For bosonic systems, the quench dynamics has been intensively studied [11–17] and can be well described by the Kibble-Zurek (KZ) theory [18, 19]. Very recently, observation of the KZ scaling was also reported in Fermi gases [20]. However, it is expected that the quench dynamics of strongly interacting Fermi systems should possess much richer physics due to the complexity of fermionic superfluid formation. Fermionic atoms have to pair into bosonic degrees of freedom, Cooper pairs or bound molecules, for the formation of a superfluid. In addition to the transition temperature  $T_c$ , there exists another characteristic temperature  $T^*$ , characterizing the onset of pair formation. In the weak coupling BCS limit, pair formation and pair condensation occur essentially at the same temperature, leading to a rapid growth of superfluid fraction as the temperature  $T$  is lowered across  $T_c$ . However, as the pairing strength increases, these two temperatures become distinct, and pairs can preform far

above  $T_c$ . This leads to a pseudogap in the fermionic excitation spectrum. At the same time, isolated superfluid islands having random relative phases may also appear above  $T_c$ . As the temperature decreases, they may merge to generate vortices spontaneously. Finally, superfluidity with global phase coherence is gradually established with the annihilation of these vortices and anti-vortices. Therefore, the quench dynamics offers a great opportunity for understanding the interplay among the formation of bosonic pairs, superfluid phase coherence, and spontaneous vortices.

Here, we report an experimental study of real-time dynamics of superfluid growth and spontaneous vortex formation in a strongly interacting Fermi gas of  ${}^6\text{Li}$  atoms. We rapidly ramp down the potential of the oblate optical trap so that the system is effectively thermally quenched across the superfluid transition. For a given ramping time, the quasi-condensate number  $N_0$  (consisting of bosonic pairs in the vicinity of zero momentum) is recorded in real time, while the spontaneously generated vortex density  $\rho_v$  is measured upon  $N_0$  reaching saturation. The observed growth dynamics of  $N_0$  agree with calculations based on the pairing fluctuation theory [21, 22], by assuming that the system temperature  $T$  decreases linearly with the evolution time  $t$  during the ramp. The pseudogap physics is clearly revealed by the evolution of the growth dynamics of  $N_0$  throughout the BCS-BEC crossover. At unitarity, for normal

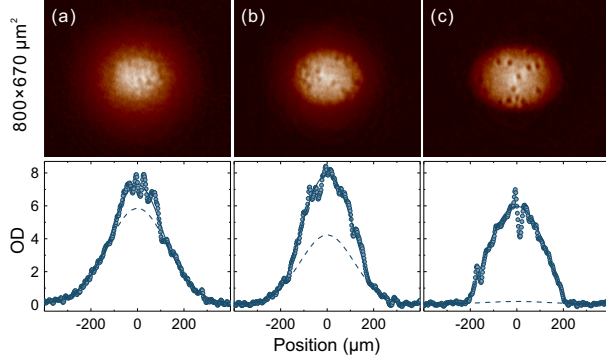


FIG. 1. Illustration of the real-time formation dynamics of quasi-condensate and spontaneous vortices, at unitarity (832 G) with  $t_{\text{ramp}} = 600$  ms. The top row shows the absorption images of the cloud after 10 ms time-of-flight (TOF) at  $t = 520$  ms, 580 ms, and 700 ms, respectively, from left to right. Here,  $t$  is defined as the evolution time of the system, i.e.,  $t = 0$  marks the start of the quench. Plots in the bottom row are central line cuts of the column density distribution. The solid lines are the fits with a Gaussian plus Thomas-Fermi distribution, and the dashed lines indicate the Gaussian part alone. The fitting yields the quasi-condensate fraction  $N_0(t)/N_{0,\text{sat}} \approx 0.1, 0.5,$  and 1 (from left to right), corresponding to the initial increase, rapid growth and saturation stages of the quasi-condensate number, respectively.

quenches with ramping time  $t_{\text{ramp}} \geq 600$  ms, the quasi-condensate formation time  $t_f$  linearly increases with  $t_{\text{ramp}}$  and the growth dynamics of  $N_0$  nicely collapse onto a single universal curve. In contrast, for fast quenches with  $t_{\text{ramp}} \leq 400$  ms,  $t_f$  drops significantly as  $t_{\text{ramp}}$  increases, and the growth curves of  $N_0$  exhibit a significant deviation from the collapse, both of which hint the breakdown of the quasi-equilibrium condition. Furthermore, by using  $t_f$  as the quench time, which is less sensitive to the pseudogap physics, a power-law scaling of  $\rho_v$  versus  $t_f$  is observed for normal quenches, and the extracted critical exponent agrees quantitatively with that predicted by the KZ theory.

The main experimental setup and method for preparing the  $^6\text{Li}$  superfluid have been described in our previous works [23]. We start by preparing a spin-balanced mixture of  $1 \times 10^7$  atoms at 832.18 G in an elliptical optical dipole trap ( $1/e^2$  radius  $200 \mu\text{m}$  and  $48 \mu\text{m}$  (in the gravity direction)). Further evaporative cooling is performed by ramping down the trap depth and holding for 3 s, yielding a superfluid of  $3.9(1) \times 10^6$  atoms at about  $0.3 T_c$ . With a short ramping time, i.e.,  $t_{\text{ramp}}$  varies from 200 ms to 1500 ms, temperature quench across the superfluid transition can be achieved, during which plenty of vortices are spontaneously generated [12, 13, 15].

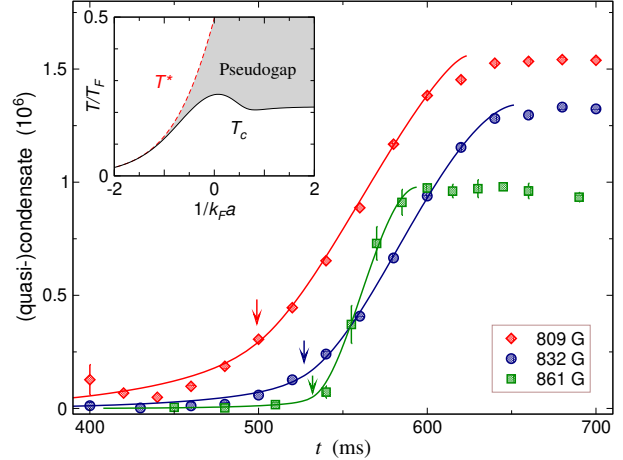


FIG. 2. Real-time dynamics of quasi-condensate number  $N_0$  with  $t_{\text{ramp}} = 600$  ms, at the magnetic field of 809 G (red diamonds, BEC side), 832 G (blue circles, unitarity) and 861 G (green squares, BCS side). Each data point is an average of about 10 individual measurements with standard statistical error. The curves represent the theoretical results calculated based on the pairing fluctuation theory, which have been re-scaled and horizontally shifted to fit the experimental data. The arrows indicate locations of superfluid transition from theory. The inset shows the phase diagram of a 3D homogeneous Fermi gas in the BCS-BEC crossover as a function of  $1/k_F a$ , which manifests a pseudogap region between  $T_c$  and  $T^*$ . Here  $k_F$  and  $a$  denote the Fermi momentum and the s-wave scattering length, respectively.

To probe the quasi-condensate and vortices, the optical trap is suddenly switched off and the magnetic field is rapidly ramped to 720 G. After expansion for a total time of 10 ms, strong saturation absorption imaging along the gravity direction is performed. The quasi-condensate number  $N_0$  is then obtained by fitting the density profile of the cloud with a Gaussian plus Thomas-Fermi distribution. The dynamic formation of vortices is clearly visible, as shown in Fig. 1. When  $N_0$  is small, the vortex cores are blurred with very low contrast and are distributed in a small spatial region. As  $N_0$  increases, the vortices become more visible and spread over the entire cloud. This gives a direct and vivid illustration of the evolution of superfluid coherence and the formation of spontaneous vortices. We mention that owing to the oblate trap geometry, the cloud expands rapidly in the gravity direction, resulting in a reduced imaging resolution. Nevertheless, upon saturation of  $N_0$ , a high contrast of vortex cores is still achieved (see Fig. 1(c)), suggesting a straight alignment of the vortex lines.

We first investigate the growth dynamics of the quasi-condensate in the BCS-BEC crossover for  $t_{\text{ramp}} =$

600 ms. Figure 2 shows the quasi-condensate number  $N_0$  as a function of  $t$  for three typical magnetic fields of 809 G, 832 G, and 861 G. Here,  $t$  is the evolution time of the system, starting at the beginning of the quench. All three  $N_0$  curves seem to have a similar shape, with an initial slow increase, followed by a rapid condensate formation, and finally a nearly flat saturation. A closer look at the growth of  $N_0$  reveals the qualitative difference as the magnetic field increases. In the initial slow increase phase,  $N_{0,\text{ini}}$  is clearly nonzero at 809 G (BEC) and 832 G (unitarity), while it remains nearly zero for 861 G (BCS). During the rapid growth stage, the formation rate of the quasi-condensate monotonically increases from the BEC to the BCS regimes.

To better understand the dependence of the  $N_0$  growth on the interaction strength (magnetic field), we numerically calculate the equilibrium quasi-condensate number  $N_0^{\text{th}}$  based on the pairing fluctuation theory [24]. The pair dispersion  $\Omega_{\mathbf{q}} \approx \hbar^2 q^2 / 2M - \mu_{\text{pair}}$ , or equivalently the effective pair mass  $M$  and the chemical potential  $\mu_{\text{pair}}$ , can be extracted from the pair propagator or the particle-particle scattering  $\mathbb{T}$  matrix. Given the temperature, interaction strength, we are able to calculate the fermionic chemical potential  $\mu$ , the pairing gap  $\Delta$ , and the superfluid order parameter  $\Delta_{\text{sc}}$  in the trap using the local density approximation. Note that the measured quasi-condensate number contains bosonic pairs with both zero and small finite momenta. Thus, we choose a small energy cutoff  $\Omega_c$ , and obtain the density profile of the quasi-condensate  $n_0(r)$  by summing over all the pairs with energy  $\hbar^2 q^2 / 2M < \Omega_c$ , i.e.,  $n_0(r) = \int_{q < \Lambda} \frac{d^3 q}{(2\pi)^3} b(\Omega_{\mathbf{q}}(r))$ , where  $b(x) = 1 / (e^{x/k_B T} - 1)$  is the Bose distribution function and the cutoff  $\Lambda = \sqrt{2M\Omega_c}$ . Here, the energy cutoff is simply taken as  $\Omega_c = k_B T / 2$ , in accordance with the experimental measurements [25]. Finally, we obtain the quasi-condensate number  $N_0 = \int d^3 r n_0(r)$  as a function of  $T$ .

To compare with the experimental growth dynamics of  $N_0$ , we assume a simple linear relation between evolution time  $t$  and temperature  $T$  before  $N_0$  saturates at very low  $T$ , especially during the condensate formation stage. The theory curves are scaled in a way to match the saturation value  $N_{0,\text{sat}}$  at low  $T$  and the slope at half saturation of their experimental counterpart. The arrows in Fig. 2 indicate the superfluid transition from theory, which correspond to a ‘‘critical time’’  $t_c$ , when the temperature crosses  $T_c$  in the evolution of the quench dynamics. It is known that, above  $T_c$ , a pseudogap in the fermionic excitation spectrum can emerge and bosonic pairs of fermionic atoms can already preform. The pair-formation temperature  $T^*$  depends on the atom-atom in-

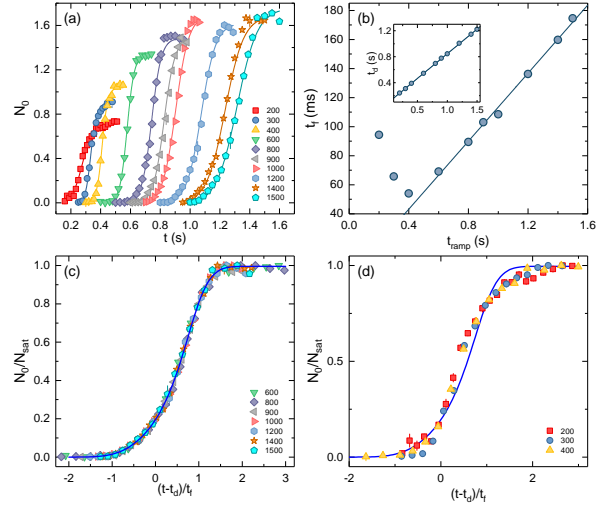


FIG. 3. Real-time dynamics of the quasi-condensate  $N_0$  at unitarity. Each data point represents an average of about 10 individual measurements with the standard error bar. (a) Growth curves with  $t_{\text{ramp}}$  ranging from 200 ms to 1500 ms, where the solid curves are guides to the eye. (b) Formation time  $t_f$  and delay time  $t_d$  (inset) versus  $t_{\text{ramp}}$ . Solid lines are linear fittings. (c)  $N_0/N_{0,\text{sat}}$  versus  $(t - t_d)/t_f$ , for normal quenches with  $t_{\text{ramp}} \geq 600$  ms. The data are fitted with a smoothing spline (solid line). (d)  $N_0/N_{0,\text{sat}}$  data for fast quenches with  $t_{\text{ramp}} \leq 400$  ms, compared with the solid curve for normal quenches.

teraction. For illustrative purpose, the phase diagram for a 3D homogeneous Fermi gas is shown in the inset of Fig. 2, where a pseudogap region is present between  $T_c$  and  $T^*$ . In general,  $T^*$  is above  $T_c$ , except in the BCS limit, where the two temperatures merge. In the unitary and the BEC regimes, a small but nonzero quasi-condensate already form before the critical time  $t_c$  or above  $T_c$ . Since the correlation length  $\xi$  is small above  $T_c$ , the superfluid coherence is yet to be established over large distances, and hence the growth of  $N_0$  is slow. As  $T$  is lowered across  $T_c$  (or equivalently  $t > t_c$ ),  $\xi$  can be as large as the linear size of the system, so that  $N_0$  enters a rapid-growth period till its saturation. In contrast, in the BCS regime, where the pseudogap is absent, the pair formation and pair condensation roughly occur at the same temperature. As a result,  $N_0$  remains nearly zero during the initial slow increase stage before entering an abrupt rapid growth immediately after  $t_c$ , as seen in the experimental data at 861 G. Therefore, our experiment clearly reveals the pseudogap physics described in the theory.

Next, we study the dependence of the quench dynamics on the ramping time  $t_{\text{ramp}}$ . Shown in Fig. 3(a) are the growth curves of  $N_0$  at unitarity for  $t_{\text{ramp}}$  ranging from

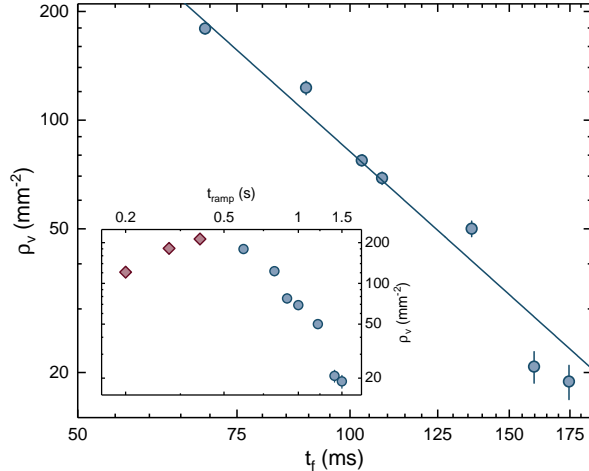


FIG. 4. Log-log plot of vortex density  $\rho_v$  versus  $t_f$ . The error bar for each point represents the standard statistical error over 30 independent measurements. The solid straight line is the power-law fitting curve based on the KZ theory. The inset shows  $\rho_v$  as a function of  $t_{\text{ramp}}$ , where blue circles and red squares denote normal and fast quenches, respectively.

200 ms to 1500 ms. As  $t_{\text{ramp}}$  becomes longer, the saturated quasi-condensate number  $N_{0,\text{sat}}$  also increases because of the less atom loss during the evaporative cooling. It is seen that for quenches with  $t_{\text{ramp}} \geq 600$  ms,  $N_0$  roughly reaches its saturation at the end of quench. In contrast, for quenches with  $t_{\text{ramp}} \leq 400$  ms, the rapid formation of  $N_0$  has barely started by  $t = t_{\text{ramp}}$ , and the much suppressed  $N_{0,\text{sat}}$  is not reached until a much later time. To better describe the quench dynamics, we introduce two time scales, delay time  $t_d$  and formation time  $t_f$ , corresponding to the starting time and the duration of the rapid formation of  $N_0$ , respectively. In practice, they are determined via  $N_0(t_d)/N_{0,\text{sat}} = 0.2$  and  $N_0(t_d + t_f)/N_{0,\text{sat}} = 0.8$ , respectively [26]. As shown in Fig. 3(b),  $t_d$  follows a nice linear increasing function of  $t_{\text{ramp}}$  for all the quenches. However, as  $t_{\text{ramp}}$  increases,  $t_f$  first decreases until it reaches a minimum around  $t_{\text{ramp}} \approx 400$  ms, and then increases linearly. Based on this observation, we classify the quenches into two types, normal and fast ones, which are separated at  $t_{\text{ramp}} \sim 500$  ms for our system. By plotting  $N_0(t)/N_{0,\text{sat}}$  versus  $(t - t_d)/t_f$ , we find that all experimental data for normal quenches can be well described by a single universal curve (see Fig. 3(c)), while those for fast quenches exhibit a significant deviation from this curve (Fig. 3(d)).

We now study the spontaneous generation of vortices in the quench dynamics, by measuring the vortex density  $\rho_v$  at the saturation of quasi-condensate for each  $t_{\text{ramp}}$ .

It is known that near the superfluid transition  $T_c$ , a diverging correlation length develops as  $\xi \sim |T - T_c|^{-\nu}$  and the relaxation time diverges as  $\tau \sim \xi^z$ , with  $\nu$  and  $z$  being the static and dynamic critical exponents, respectively [18, 19]. Under the condition that the temperature  $T$  varies linearly with time near  $T_c$ , the KZ theory predicts that  $\rho_v$  decays algebraically with the quench rate  $1/\tau_Q$  as  $\rho_v \sim \tau_Q^{-\alpha_{\text{KZ}}}$ , where the exponent  $\alpha_{\text{KZ}}$  is determined by  $\nu$  and  $z$ . Experimentally, the measurement of temperature evolution in quench dynamics is a great challenge for strongly interacting Fermi gases. In previous studies,  $\tau_Q \sim t_{\text{ramp}}$  has been reported [13, 20, 27, 28], and thus we first attempt to plot  $\rho_v$  versus  $t_{\text{ramp}}$ . As shown in the inset of Fig. 4, an approximate power-law decay is observed for normal quenches, while for fast quenches the  $t_{\text{ramp}}$  dependence of  $\rho_v$  clearly deviates from the KZ scaling.

To understand the normal and fast quenches better, we revisit the relaxation dynamics of an out-of-equilibrium system. For a superfluid, there are two types of excitations, i.e., low-energy density waves and high-energy vortices. Typically, the relaxation of low energy modes is much faster than the annihilation of vortex and anti-vortex pairs. The quasi-equilibrium condition is assumed that, at each evolution time, the low energy modes have been sufficiently relaxed while the vortices remain excited. For normal quenches, the quasi-equilibrium condition is supported by the observations that the formation time  $t_f$  of the quasi-condensate increases linearly with  $t_{\text{ramp}}$  (see Fig. 3(b)),  $N_0$  almost reaches  $N_{0,\text{sat}}$  at the end of the quench, and that the saturated vortex density  $\rho_v$  decays algebraically. On the other hand, the unusual  $t_{\text{ramp}}$  dependence of  $t_f$  and  $\rho_v$ , as well as the barely started growth of  $N_0$  by  $t = t_{\text{ramp}}$ , suggest that the quasi-equilibrium condition is broken for fast quenches.

In Fig. 4, the data points of  $\rho_v$  versus  $t_f$  for normal quenches agree well with a power-law scaling. Indeed,  $t_f$  reflects the linear growth period of  $N_0$  and the linear decrease of temperature with time. Unlike  $t_{\text{ramp}}$ , it is insensitive to the (somewhat arbitrary) initial temperature of the system ( $T$  at  $t = 0$ ) as well as the complications caused by the pair formation process during the slow incubation stage. Therefore, it is inversely proportional to the quench rate near  $T_c$  and thus may naturally play the role of  $\tau_Q$  in the KZ theory. Fitting the experimental data with a power-law function  $\rho_v \sim t_f^{-\alpha_{\text{KZ}}}$ , we obtain the KZ exponent  $\alpha_{\text{KZ}} = 2.25(17)$ . In a 3D harmonic trap, the KZ exponent has been predicted to be  $\alpha_{\text{KZ}} = 2(1 + 2\nu)/(1 + \nu z)$  [29, 30]. According to the F model,  $\nu = 2/3$  and  $z = 3/2$  for a 3D system [31], which yields  $\alpha_{\text{KZ}} = 7/3$ . Our experimental result is in quantitative agreement with this theoretical value, demonstrating



the validity of using  $t_f$  to characterize the quench rate for normal quenches.

In conclusion, we have studied the quench dynamics of a strongly interacting atomic Fermi gas by ramping down the trapping potential. Our experiment directly demonstrates the interplay between the real-time dynamics of quasi-condensate growth and spontaneous vortex formation. Comparison between theoretical calculations and experimental data reveals the pseudogap physics, which leads to significant differences in the growth dynamics of quasi-condensate between the BEC and BCS regimes. We find that the quench processes can be classified into normal and fast quenches. The unusual non-monotonic  $t_{\text{ramp}}$  dependence of the quasi-condensate formation time  $t_f$  and the vortex density  $\rho_v$  suggests that the quasi-equilibrium condition is broken during the fast quench processes. For normal quenches, by using  $t_f$  to characterize the quench time of the system, the KZ scaling of strongly interacting Fermi gas is observed and the extracted KZ exponent agrees well with the theoretical prediction. Our work may serve as a starting point for exploring rich quantum phenomena of quasi-2D vortices, such as Berezinskii-Kosterlitz-Thouless physics in a quasi-2D trap [32], holographic liquids [33], and quantum turbulence [34–36].

This work is supported by the National Key R&D Program of China (Grant Nos. 2018YFA0306501, 2017YFA0304204, 2016YFA0301604), NSFC of China (Grant Nos. 11874340, 11425417, 11774067, 11774309, 11625522, 11934002), the Chinese Academy of Sciences (CAS), the Anhui Initiative in Quantum Information Technologies, the Shanghai Municipal Science and Technology Major Project (Grant No.2019SHZDZX01).

---

\* These authors contributed equally to this work.

- [1] Immanuel Bloch, Jean Dalibard, and Wilhelm Zwerger, “Many-body physics with ultracold gases,” *Rev. Mod. Phys.* **80**, 885–964 (2008).
- [2] Stefano Giorgini, Lev P. Pitaevskii, and Sandro Stringari, “Theory of ultracold atomic fermi gases,” *Rev. Mod. Phys.* **80**, 1215–1274 (2008).
- [3] Cheng Chin, Rudolf Grimm, Paul Julienne, and Eite Tiesinga, “Feshbach resonances in ultracold gases,” *Rev. Mod. Phys.* **82**, 1225–1286 (2010).
- [4] Tilman Esslinger, “Fermi-hubbard physics with atoms in an optical lattice,” *Annu. Rev. Condens. Matter Phys.* **1**, 129–152 (2010).
- [5] Qijin Chen and Jibiao Wang, “Pseudogap phenomena in ultracold atomic fermi gases,” *Frontiers of Physics* **9**, 539–570 (2014).
- [6] Erich J Mueller, “Review of pseudogaps in strongly interacting fermi gases,” *Rep. Prog. Phys.* **80**, 104401 (2017).
- [7] Tom Timusk and Bryan Statt, “The pseudogap in high-temperature superconductors: an experimental survey,” *Rep. Prog. Phys.* **62**, 61–122 (1999).
- [8] Patrick A. Lee, Naoto Nagaosa, and Xiao-Gang Wen, “Doping a mott insulator: Physics of high-temperature superconductivity,” *Rev. Mod. Phys.* **78**, 17–85 (2006).
- [9] Patrick A Lee, “From high temperature superconductivity to quantum spin liquid: progress in strong correlation physics,” *Rep. Prog. Phys.* **71**, 012501 (2007).
- [10] G. Baym, C. Pethick, and D. Pines, “Superfluidity in neutron stars,” *Nature* **224**, 673–674 (1969).
- [11] L. E. Sadler, J. M. Higbie, S. R. Leslie, M. Vengalattore, and D. M. Stamper-Kurn, “Spontaneous symmetry breaking in a quenched ferromagnetic spinor bose–einstein condensate,” *Nature* **443**, 312–315 (2006).
- [12] Chad N. Weiler, Tyler W. Neely, David R. Scherer, Ashton S. Bradley, Matthew J. Davis, and Brian P. Anderson, “Spontaneous vortices in the formation of bose–einstein condensates,” *Nature* **455**, 948–951 (2008).
- [13] Giacomo Lamporesi, Simone Donadello, Simone Serafini, Franco Dalfovo, and Gabriele Ferrari, “Spontaneous creation of kibble–zurek solitons in a bose–einstein condensate,” *Nat. Phys.* **9**, 656–660 (2013).
- [14] L. Corman, L. Chomaz, T. Bienaimé, R. Desbuquois, C. Weitenberg, S. Nascimbène, J. Dalibard, and J. Beugnon, “Quench-induced supercurrents in an annular bose gas,” *Phys. Rev. Lett.* **113**, 135302 (2014).
- [15] N. Navon, A. L. Gaunt, R. P. Smith, and Z. Hadzibabic, “Critical dynamics of spontaneous symmetry breaking in a homogeneous bose gas,” *Science* **347**, 167–170 (2015).
- [16] Lauriane Chomaz, Laura Corman, Tom Bienaimé, Rémi Desbuquois, Christof Weitenberg, Sylvain Nascimbène, Jérôme Beugnon, and Jean Dalibard, “Emergence of coherence via transverse condensation in a uniform quasi-two-dimensional bose gas,” *Nat. Commun.* **6** (2015), 10.1038/ncomms7162.
- [17] M. Anquez, B. A. Robbins, H. M. Bharath, M. Boguslawski, T. M. Hoang, and M. S. Chapman, “Quantum kibble-zurek mechanism in a spin-1 bose-einstein condensate,” *Phys. Rev. Lett.* **116**, 155301 (2016).
- [18] T W B Kibble, “Topology of cosmic domains and strings,” *J. Phys. A: Math. Gen.* **9**, 1387–1398 (1976).
- [19] W. H. Zurek, “Cosmological experiments in superfluid helium?” *Nature* **317**, 505–508 (1985).
- [20] Bumsuk Ko, Jee Woo Park, and Y. Shin, “Kibble–zurek universality in a strongly interacting fermi superfluid,” *Nat. Phys.* **15**, 1227–1231 (2019).
- [21] Q J Chen, I Kosztin, B Jankó, and K Levin, “Pairing fluctuation theory of superconducting properties in underdoped to overdoped cuprates.” *Phys. Rev. Lett.* **81**, 4708–11 (1998).
- [22] Q J Chen, J Stajic, S N Tan, and K Levin, “BCS-BEC crossover: From high temperature superconductors to ultracold superfluids,” *Phys. Rep.* **412**, 1–88 (2005).
- [23] Xing-Can Yao, Hao-Ze Chen, Yu-Ping Wu, Xiang-Pei Liu, Xiao-Qiong Wang, Xiao Jiang, Youjin Deng, Yu-Ao Chen, and Jian-Wei Pan, “Observation of coupled vortex lattices in a mass-imbalance bose and fermi superfluid

- mixture,” *Phys. Rev. Lett.* **117**, 145301 (2016).
- [24] Qijin Chen, Jelena Stajic, and K. Levin, “Thermodynamics of Interacting Fermions in Atomic Traps,” *Phys. Rev. Lett.* **95**, 260405 (2005).
- [25] For qualitative comparison between experiment and theory, fine-tuning of  $\Omega_c$  is not necessary.
- [26] Note that slight variation in the cutoff percentages does not change the power law exponent in the KZ scaling in Fig. 4.
- [27] S. Donadello, S. Serafini, T. Bienaimé, F. Dalfovo, G. Lamporesi, and G. Ferrari, “Creation and counting of defects in a temperature-quenched bose-einstein condensate,” *Phys. Rev. A* **94**, 023628 (2016).
- [28] After our manuscript was submitted, a recent preprint appeared online as arXiv:2105.06601 by J. Goo, Y. Lim and Y. Shin.
- [29] Wojciech H. Zurek, “Causality in condensates: Gray solitons as relics of BEC formation,” *Phys. Rev. Lett.* **102**, 105702 (2009).
- [30] A del Campo, A Retzker, and M B Plenio, “The inhomogeneous kibble–zurek mechanism: vortex nucleation during bose–einstein condensation,” *New J. Phys.* **13**, 083022 (2011).
- [31] P. C. Hohenberg and B. I. Halperin, “Theory of dynamic critical phenomena,” *Rev. Mod. Phys.* **49**, 435–479 (1977).
- [32] V L Berezinskii, “Destruction of long-range order in one dimensional and two dimensional systems possessing a continuous symmetry group II. Quantum systems,” *Sov. Phys. JETP* **34**, 610 (1972), *zh. Eksp. Teor. Fiz.* 61(3), 1144-1156 (1971); J M Kosterlitz and D J Thouless, “Ordering, metastability and phase transitions in two dimensional systems,” *J. Phys. C. Solid State* **6**, 1181 (1973).
- [33] P. M. Chesler, H. Liu, and A. Adams, “Holographic vortex liquids and superfluid turbulence,” *Science* **341**, 368–372 (2013).
- [34] Makoto Tsubota, “Quantum turbulence: from superfluid helium to atomic bose–einstein condensates,” *Contemp. Phys.* **50**, 463–475 (2009).
- [35] C. F. Barenghi, L. Skrbek, and K. R. Sreenivasan, “Introduction to quantum turbulence,” *Proc. Nat. Acad. Sci.* **111**, 4647–4652 (2014).
- [36] Aurel Bulgac, Michael McNeil Forbes, and Gabriel Włazłowski, “Towards quantum turbulence in cold atomic fermionic superfluids,” *J. Phys. B: At., Mol. Opt. Phys.* **50**, 014001 (2016).